Shuanliang Zhang, Huayong Chen, Pete Hollings, Liandang Zhao, and Lin Gong, 2020, Tectonic and magmatic evolution of the Aqishan-Yamansu belt: A Paleozoic arc-related basin in the Eastern Tianshan (NW China): GSA Bulletin, https://doi.org/10.1130/B35749.1.

Supplemental Material

TABLE S1. LA-ICP-MS zircon U-Pb data for volcanic/volcaniclastic rocks and intrusions samples from the Shuanglong area in the Aqishan-Yamansu belt, Eastern Tianshan.

TABLE S2. The whole-rock major (wt%) and trace elements (ppm) of volcanic/volcaniclastic rocks and intrusions samples from the Shuanglong area in the Aqishan-Yamansu belt, Eastern Tianshan.

TABLE S3. The whole-rock Sr-Nd isotopes results of volcanic/volcaniclastic rocks and intrusions samples from the Shuanglong area in the Aqishan-Yamansu belt, Eastern Tianshan.

TABLE S4. Summary of geochemistry data for the magmatism in the Aqishan-Yamansu belt, Eastern Tianshan.

TABLE S5. Summary of geological data for the magmatism in the Aqishan-Yamansu belt, Eastern Tianshan.

TABLE S6. Summary of whole-rock Sr-Nd isotopes data for the magmatism in the Aqishan-Yamansu belt, Eastern Tianshan.

FIGURE S1. The cathodoluminescence (CL) images of zircons and the corresponding $^{206}Pb/^{238}U$ ages for volcanic/volcaniclastic rocks and intrusions samples from the Shuanglong area in the Aqishan-Yamansu belt, Eastern Tianshan.

FIGURE S2. Plots of U/Sc versus U (A) and Rb versus La (B) for the quartz diorite and diorite porphyry from the Shuanglong area in the Aqishan-Yamansu belt.

FIGURE S3. Field photos of the pre-mineralization EW-strike reverse fault in the Shuanglong Fe-Cu deposit district.

Color versions of Figure 2, Figure 3, Figure 4, and Figure 17.

REFERENCES CITED

Dai, A., 2015, Study on the Geological Characteristics and the Genesis of the Bailingshan Iron Deposit in Eastern Tianshan, Xinjiang Province [Master's thesis]: Xi'an, China, Chang'an University, 59 p. [in Chinese with English abstract].

Dai, J. F., Xue, C. J., Chi, G. X., Gao, R. Z., Ming, H., Zhao, X. B., and Zhao, Y., 2020, Genesis of the Aqishan skarn Zn-Pb deposit in the Eastern Tianshan, NW China: Constraints from geology, geochronology and Hf-S-Pb isotopic geochemistry: Ore Geology Reviews, v. 123, p. 15, https://doi.org/10.1016/j.oregeorev.2020.103608.

Du, L., Long, X., Yuan, C., Zhang, Y., Huang, Z., Wang, X., and Yang, Y., 2018, Mantle contribution and tectonic transition in the Aqishan-Yamansu belt, Eastern Tianshan, NW China: Insights from geochronology and geochemistry of early Carboniferous to early Permian felsic intrusions: Lithos, v. 304–307, p. 230–244, https://doi.org/10.1016/j.lithos.2018.02.010.

Huang, X., Qi, L., Gao, J., Liu, Y., and Wang, Y., 2012, Geochemistry of volcanic rocks in the Dikan'er Formation of Jueluotage region, Eastern Tianshan Mountains, and its tectonic implications: Acta Petrologica et Mineralogica, v. 31, no. 6, p. 799–817 [in Chinese with English abstract].

Jiang, H., Han, J., Chen, H., Zheng, Y., Lu, W., Deng, G., and Tan, Z., 2017, Intra-continental back-arc basin inversion and late Carboniferous magmatism in Eastern Tianshan, NW China: Constraints from the Shaquanzi magmatic suite: Geoscience Frontiers, v. 8, no. 6, p. 1447–1467, https://doi.org/10.1016/j.gsf.2017.01.008.

Lei, R., ChangZhi, W., ZunZhong, Z., Lianxing, G., Junhua, T., and Guangrong, L., 2013, Geochronology, geochemistry and tectonic significances of the Yamansubei pluton in eastern Tianshan, Northwest China: Acta Petrologica Sinica, v. 29, no. 8, p. 2653-2664 [in Chinese with English abstract].

Li, W., Ren, B., Yang, X., Li, Y., and Chen, Q., 2002, The intermediate-acid intrusive magmatism and its geodynamic significance in Eastern Tianshan region: Northwestern Geology, v. 35, no. 4, p. 41-64 [in Chinese with English abstract].

Li, Y., Jingsui, Y., Jian, Z., Tianfu, L., Songyong, C., YuFeng, R., and XiangZhen, X., 2011, Tectonic significance of the Carboniferous volcanic rocks in eastern Tianshan: Acta Petrologica Sinica (Yanshi Xuebao), v. 27, no. 1, p. 193–209 [in Chinese with English abstract].

Long, X., Wu, B., Sun, M., Yuan, C., Xiao, W., and Zuo, R., 2019, Geochronology and geochemistry of Late Carboniferous dykes in the Aqishan–Yamansu belt, eastern Tianshan: Evidence for a post-collisional slab breakoff: Geoscience Frontiers, https://doi.org/10.1016/j.gsf.2019.06.003.

Luo, T., Liao, Q.-A., Chen, J.-P., Zhang, X.-H., Guo, D.-B., and Hu, Z.-C., 2012, LA-ICP-MS zircon U-Pb dating of the volcanic rocks from Yamansu Formation in the Eastern Tianshan, and its geological significance: Earth Science (Diqiu Kexue), v. 37, no. 6 [in Chinese with English abstract].

Luo, T., Liao, Q.-A., Zhang, X.-H., Chen, J.-P., Wang, G.-C., and Huang, X., 2015, Geochronology and geochemistry of Carboniferous metabasalts in eastern Tianshan, Central Asia: evidence of a back-arc basin: International Geology Review, v. 58, no. 6, p. 756-772, https://doi.org/10.1080/00206814.2015.1114433.

Su, C., Jiang, C., Xia, M., Wei, W., and Pan, R., 2009, Geochemistry and zircons SHRIMP U-Pb age of volcanic rocks of Aqishan Formation in the eastern area of north Tianshan, China: Acta Petrologica Sinica (Yanshi Xuebao), v. 25, no. 4, p. 901–915 [in Chinese with English abstract].

Sun, Z. Y., Wang, J. B., Wang, Y. W., Long, L. L., Luo, Z. H., Deng, X. H., Hu, Q. T., and Wang, M. L., 2020, Sodium-rich volcanic rocks and their relationships with iron deposits in the Aqishan-Yamansu belt of Eastern Tianshan, NW China: Geoscience Frontiers, v. 11, no. 2, p. 697-713, https://doi.org/10.1016/j.gsf.2019.06.011.

Wang, Y.-H., Xue, C.-J., Gao, J.-B., Zhang, F.-F., Liu, J.-J., Wang, J.-P., and Wang, J.-C., 2016, The genesis of the ores and granitic rocks at the Hongshi Au deposit in Eastern Tianshan, China: Constraints from zircon U–Pb geochronology, geochemistry and isotope systematics: Ore Geology Reviews, v. 74, p. 122-138, https://doi.org/10.1016/j.oregeorev.2015.11.018.

Wang, L., Li, H., Chen, Y., and Liu, D., 2005, Geological feature and mineralization epoch of Bailingshan iron deposit, Hami, Xin-jiang, China: MINERAL DEPOSITS-BEIJING-, v. 24, no. 3, p. 264 [in Chinese with English abstract].

Wu, C.Z., Zhang, Z.Z., Zaw, K., Della-Pasque, F., Tang, J.H., Zheng, Y.C., Wang, C.S., and San, J.Z., 2006, Geochronology, geochemistry and tectonic significances of the Hongyuntan granitoids in the Qoltag area, Eastern Tianshan: Acta Petrologica Sinica (Yanshi Xuebao), v. 22, no. 5, p. 1121–1134 [in Chinese with English abstract].

Wu, B., 2019, Late Paleozoic Magmatism and Crustal Growth in the Aqishan-Yamansu Belt of Eastern Tianshan [Master's thesis]: Xi'an, China, Northwest University, 111 p. [in Chinese with English abstract].

Xu, L., Chai, F., Li, Q., Zeng, H., Geng, X., Xia, F., and Deng, G., 2014, Geochemistry and zircon U-Pb age of volcanic rocks from the Shaquanzi Fe-Cu deposit in East Tianshan Mountains and their geological significance: Geology in China, v. 41, no. 6, p. 1771–1790 [in Chinese with English abstract].

Zhang, D.Y., 2012, Petrogenesis, Mineralization and Geodynamic Evolution in Jueluotage Area, Eastern Tianshan, Northwest China [Ph.D. thesis]: Hefei, China, Hefei University of Technology, 217 p. [in Chinese with English abstract].

Zhang, D.Y., Zhou, T.F., Yuan, F., Fiorentini, M.L., Said, N., Lu, Y.J., and Pirajno, F., 2013, Geochemical and isotopic constraints on the genesis of the Jueluotage native copper mineralized basalt, Eastern Tianshan, Northwest China: Journal of Asian Earth Sciences, v. 73, p. 317–333, https://doi.org/10.1016/j.jseaes.2013.04.043.

Zhang, W., Chen, H., Han, J., Zhao, L., Huang, J., Yang, J., and Yan, X., 2016, Geochronology and geochemistry of igneous rocks in the Bailingshan area: Implications for the tectonic setting of late Paleozoic magmatism and iron skarn mineralization in the Eastern Tianshan, NW China: Gondwana Research, v. 38, p. 40–59, https://doi.org/10.1016/j.gr.2015.10.011.

Zhang, W., Chen, H., Jiang, H., Lu, W., Liang, P., Xu, C., Yan, X., and Yang, J., 2017, Geochronology, geochemistry and petrogenesis of granitoids in the Duotoushan Fe-Cu deposit, Eastern Tianshan, Xinjiang Province: Implications on tectonic setting of late Paleozoic magmatism: Geotectonica et Metallogenia, v. 14, p. 1171–1191 [in Chinese with English abstract].

Zhao, L., Chen, H., Zhang, L., Zhang, W., Yang, J.T., and Yan, X.L., 2018, The late Paleozoic magmatic evolution of the Aqishan-Yamansu belt, Eastern Tianshan: Constraints from geochronology, geochemistry and Sr-Nd-Pb-Hf isotopes of igneous rocks: Journal of Asian Earth Sciences, v. 153, p. 170–192, https://doi.org/10.1016/j.jseaes.2017.07.038.

Zhao, L., Chen, H., and Hollings, P., 2019a, Tectonic transition in the Aqishan-Yamansu belt, Eastern Tianshan: Constraints from the geochronology and geochemistry of Carboniferous and Triassic igneous rocks: Lithos, v. 344–345, p. 247–264, https://doi.org/10.1016/j.lithos.2019.06.023.

Zhao, L., Chen, H., Hollings, P., and Han, J., 2019b, Late Paleozoic magmatism and metallogenesis in the Aqishan-Yamansu belt, Eastern Tianshan: Constraints from the Bailingshan intrusive complex: Gondwana Research, v. 65, p. 68–85, https://doi.org/10.1016/j.gr.2018.08.004.

Zheng, R., 2015, Geological Characteristics and Genesis of Hongyuntan Iron Deposits in the Eastern Tianshan, Xinjiang [Master's thesis]: Beijing, China, China University of Geosciences, 114 p. [in Chinese with English abstract].

Zhou, T., Yuan, F., Zhang, D., Fan, Y., Liu, S., Peng, M., and Zhang, J., 2010, Geochronology, tectonic setting and mineralization of granitoids in Jueluotage area, eastern Tianshan, Xinjiang: Acta Petrologica Sinica (Yanshi Xuebao), v. 26, no. 2, p. 478-502 [in Chinese with English abstract].

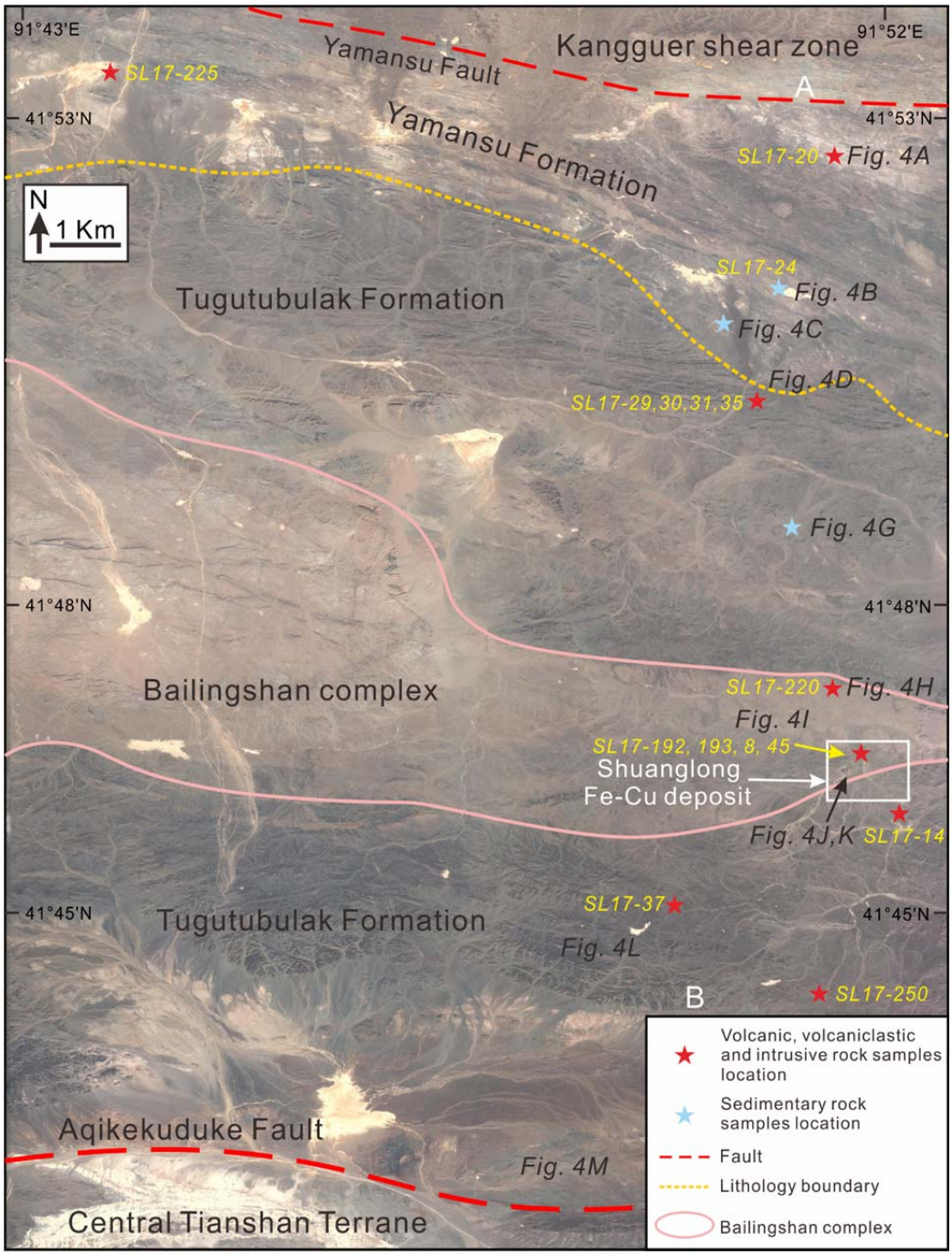

Figure 2. Satellite imagery of the study area in the Aqishan-Yamansu belt, Eastern Tianshan (Shanshan County, China). Retrieved from Google Maps (https://www.google.com/maps/@41.8010838,91.7811642,19001m/data=!3m1!1e3?hl=zh-CN).

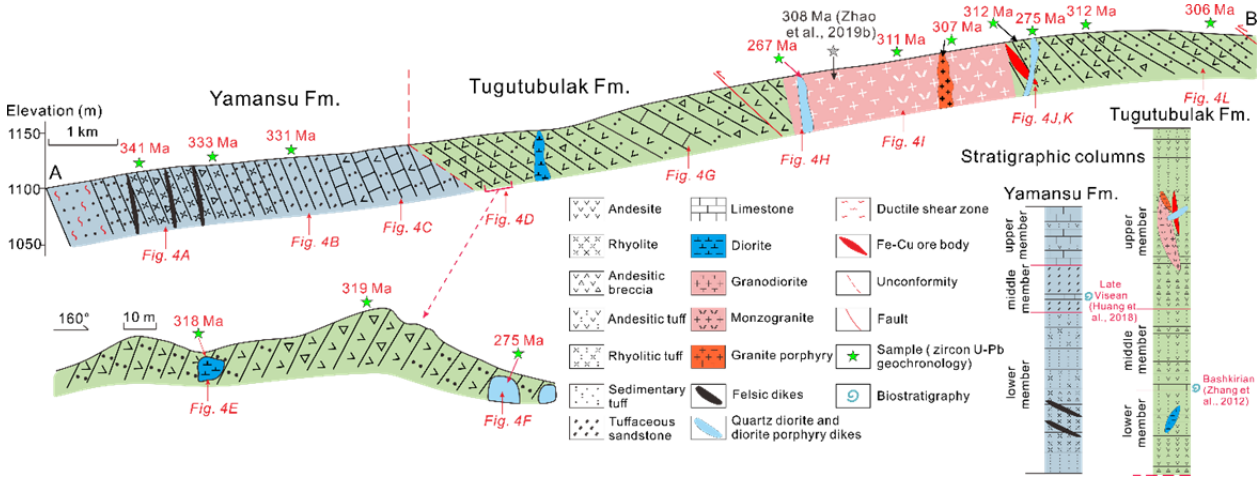

Figure 3. Geological cross-section A–B and simplified stratigraphic columns of the Carboniferous strata in the Aqishan-Yamansu belt.

Figure 4. Field photos of Carboniferous strata in the Aqishan-Yamansu belt, intrusions, and the Shuanglong Fe-Cu deposit. (A) Panoramic view of the boundary between the Aqishan-Yamansu belt and the Kangguer shear zone, and the lower Yamansu Formation rhyolite and the obsidian dikes. (B) Tuffaceous sandstone in the middle Yamansu Formation. (C) Limestone intercalations in the upper Yamansu Formation. (D) Panoramic view of the boundary between the upper Yamansu Formation and the lower Tugutubulak Formation. (E) Diorite intruded into the andesitic tuff of the Tugutubulak Formation. (F) Diorite porphyry intruded into the andesite of the Tugutubulak Formation. (G) Limestone in the middle Tugutubulak Formation. (H–I) The granodiorite, monzogranite, and quartz diorite intrusions. (J–K) Shuanglong Fe-Cu mineralization and the orebody cut by the diorite porphyry intrusion. (L) Sedimentary tuff and amygdaloidal andesite in the upper Tugutubulak Formation. (M) Aqikekuduke fault.

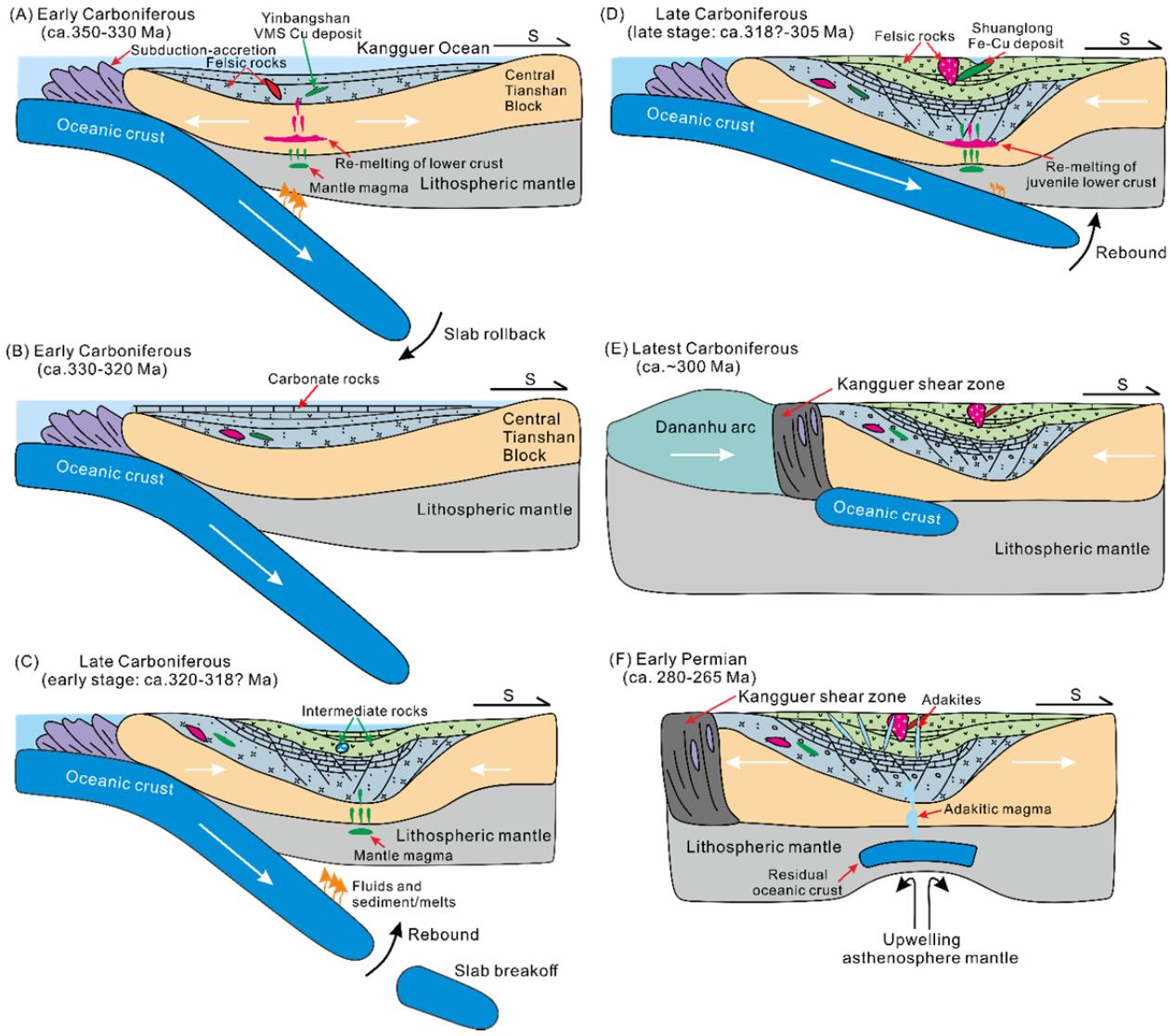

Figure 17. Tectonic-magmatic-metallogenic models of the Aqishan-Yamansu belt in the Eastern Tianshan during the Carboniferous to Permian. VMS—volcanogenic massive sulfide.

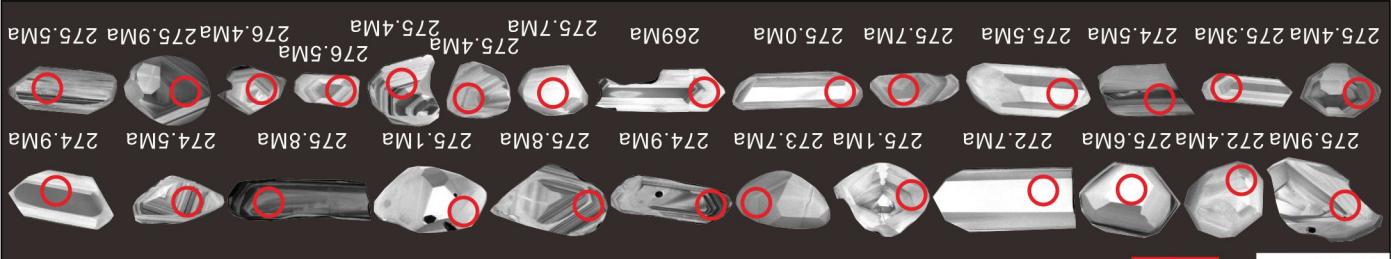

SL17-14 100μm

SL17-30 100μm

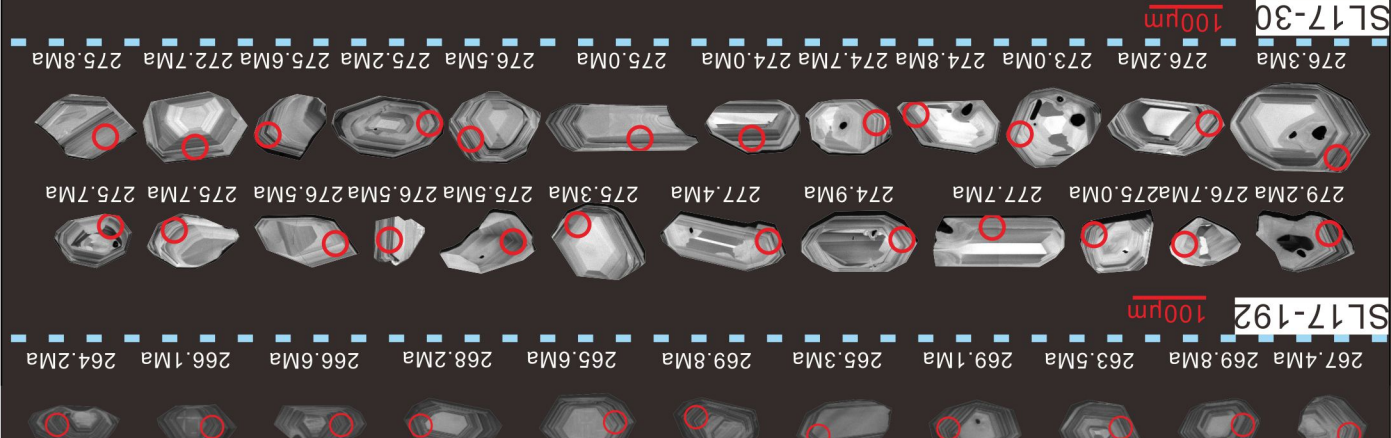

SL17-192 100μm

SL17-220 100μm

SL17-8 100μm

SL17-193 100μm

SL17-31 100μm

SL17-37 100μm

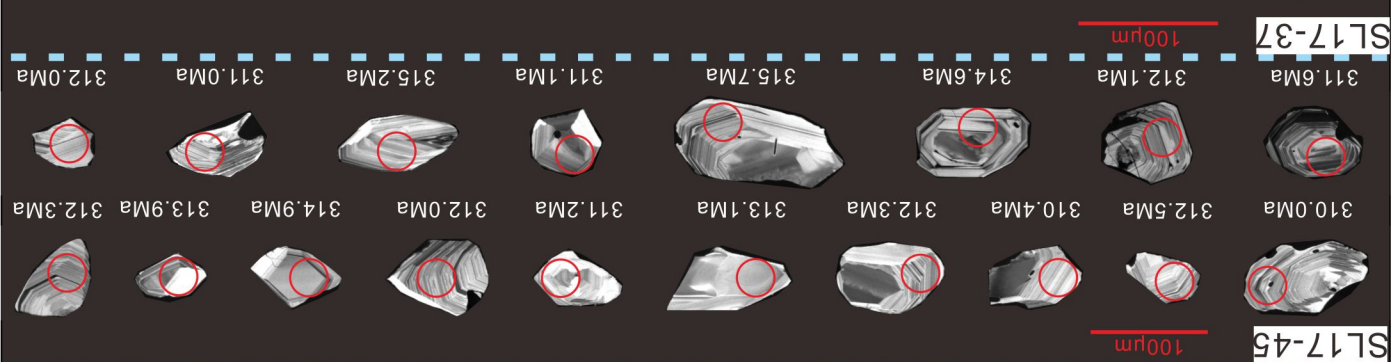

SL17-45 100μm

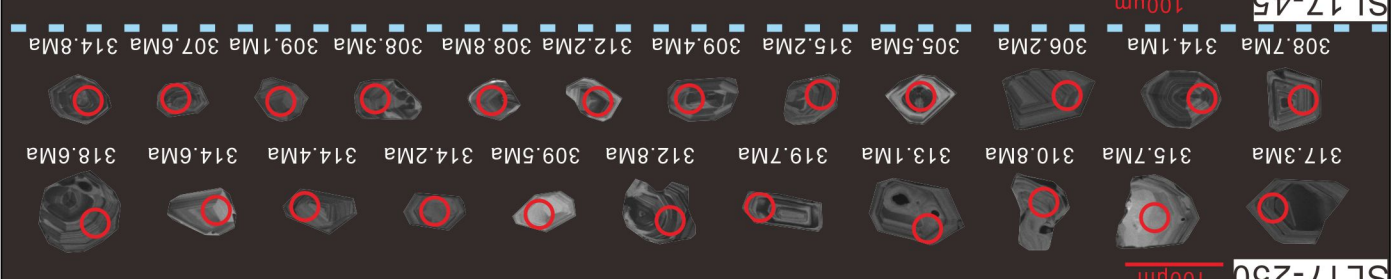

SL17-250 100μm

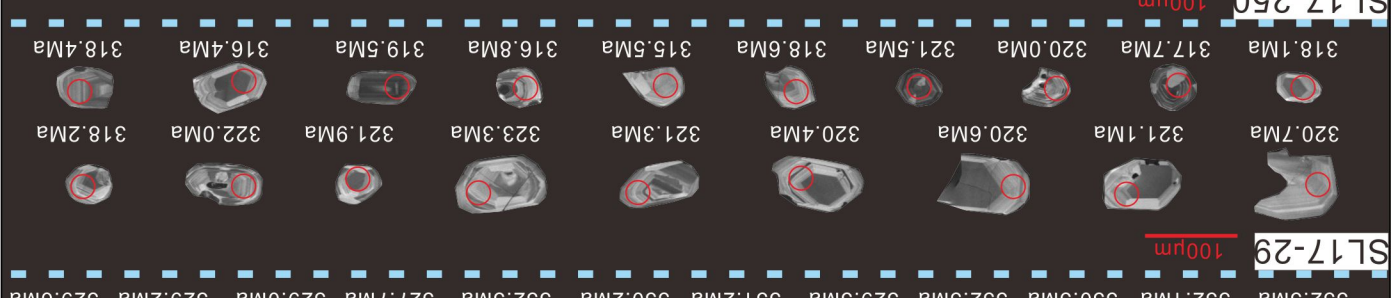

SL17-29 100μm

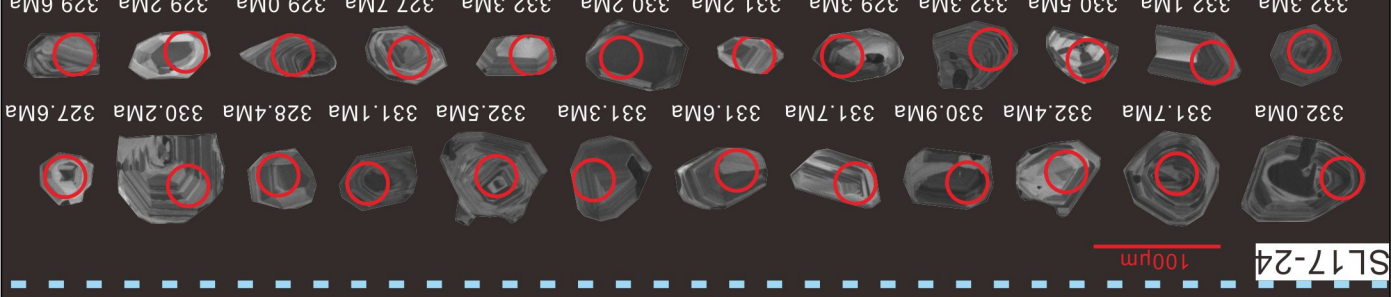

SL17-24 100μm

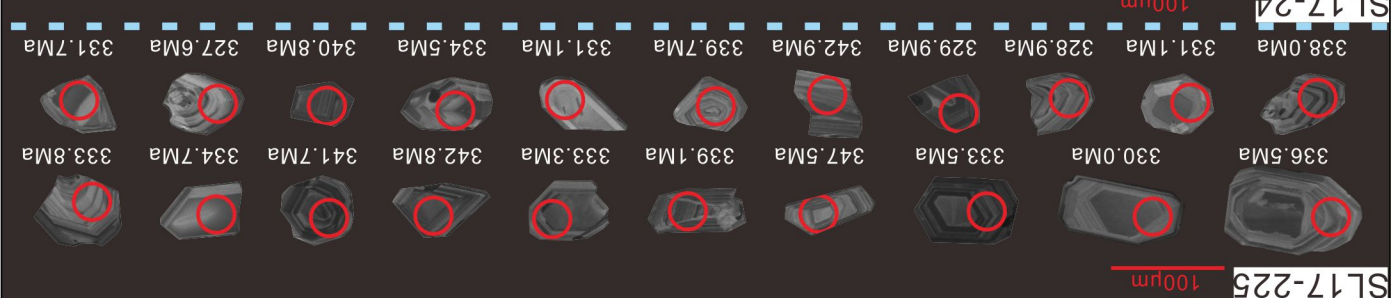

SL17-225 100μm

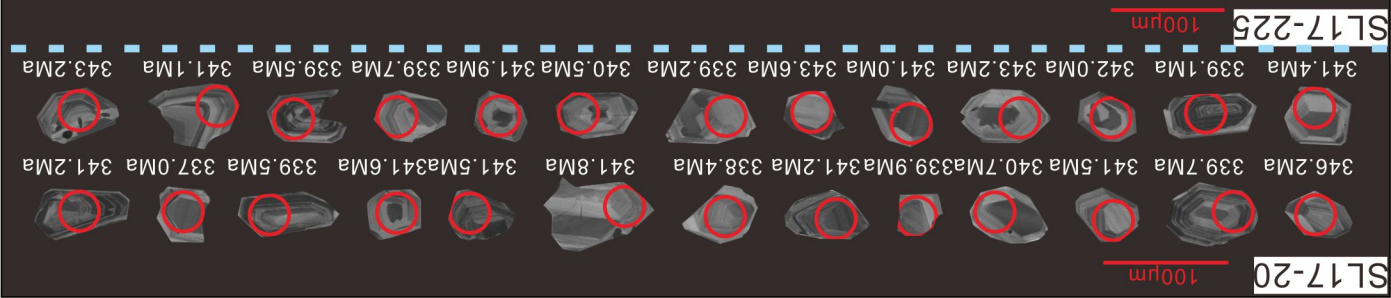

SL17-20 100μm

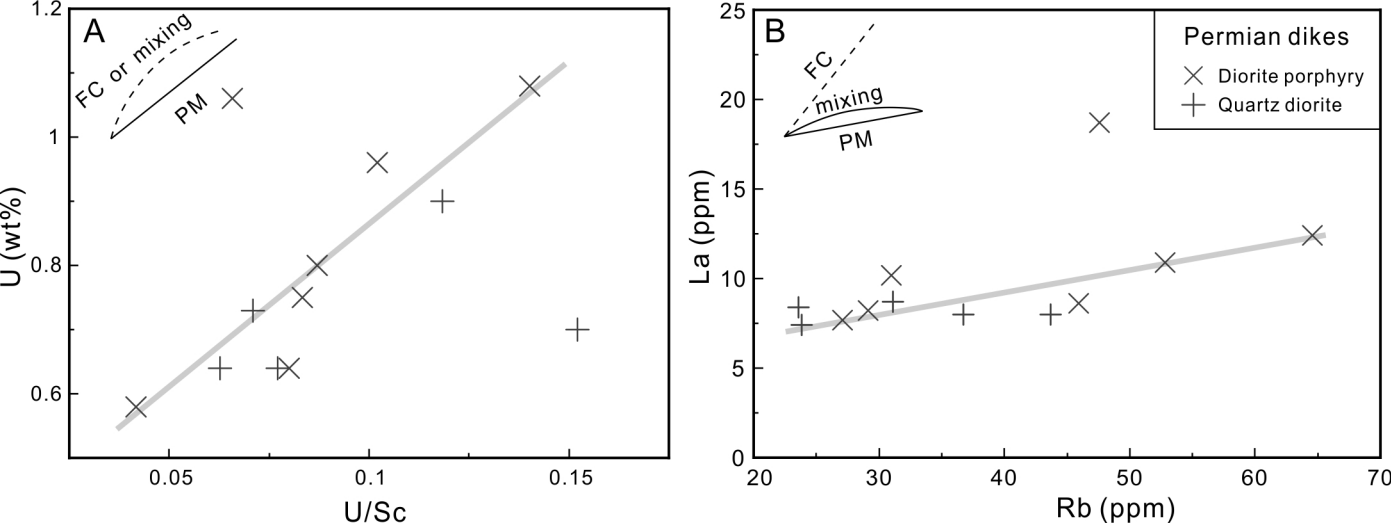
A
FC or mixing
PM
U (wt%)
U/Sc
1.2
1
0.8
0.6
0.05
0.1
0.15
B
FC
mixing
PM
Permian dikes
Diorite porphyry
Quartz diorite
La (ppm)
Rb (ppm)
25
20
15
10
5
0
20
30
40
50
60
70

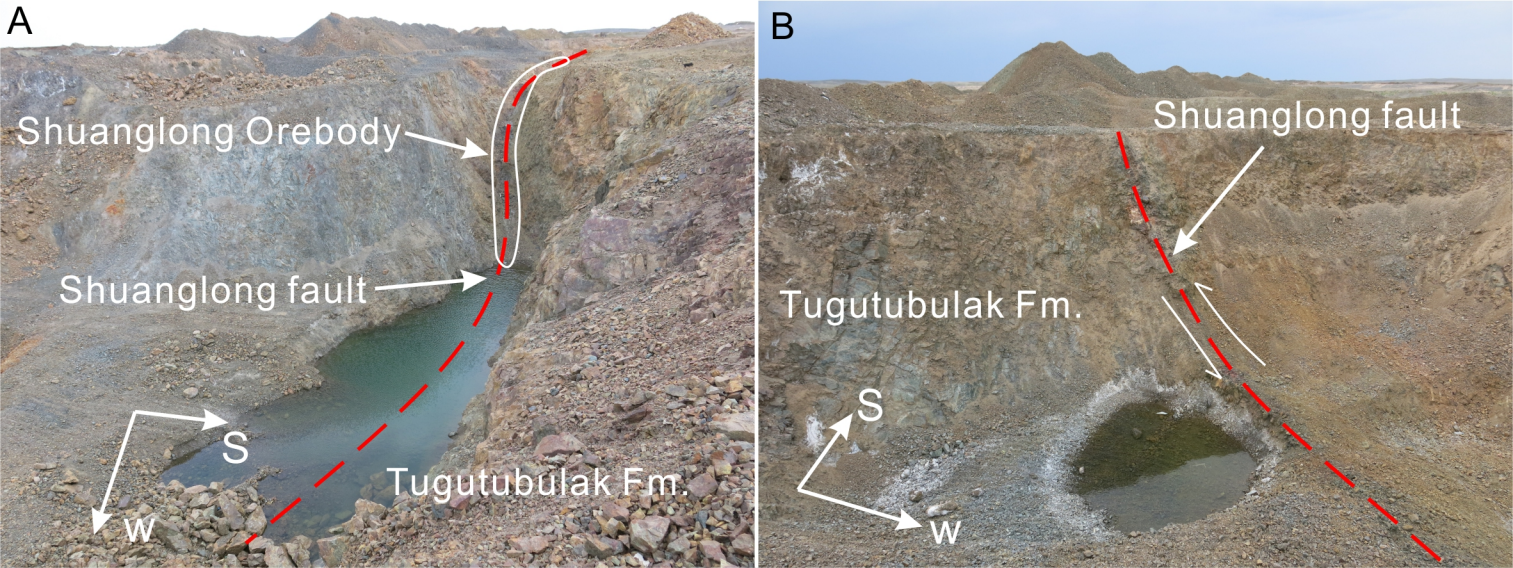
A
Shuanglong Orebody
Shuanglong fault
S
W
Tugutubulak Fm.
B
Shuanglong fault
Tugutubulak Fm.
S
W

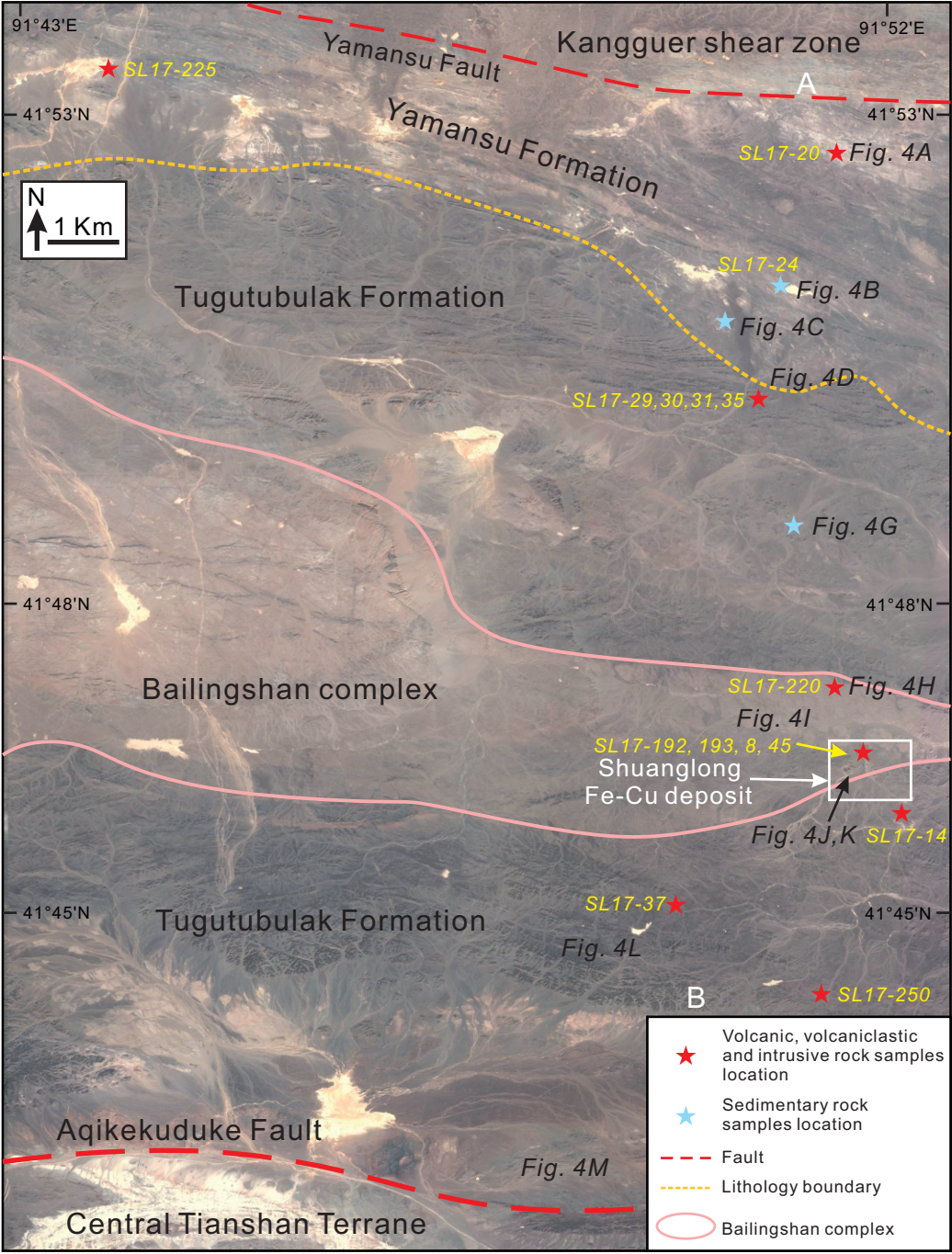
91°43'E
91°52'E
Yamansu Fault
Kangguer shear zone
A
SL17-225
41°53'N
41°53'N
Yamansu Formation
SL17-20
Fig. 4A
N
1 Km
SL17-24
Fig. 4B
Tugutubulak Formation
Fig. 4C
Fig. 4D
SL17-29,30,31,35
Fig. 4G
41°48'N
41°48'N
Bailingshan complex
SL17-220
Fig. 4H
Fig. 4I
SL17-192, 193, 8, 45
Shuanglong
Fe-Cu deposit
Fig. 4J,K
SL17-14
41°45'N
Tugutubulak Formation
SL17-37
41°45'N
Fig. 4L
B
SL17-250
Volcanic, volcaniclastic and intrusive rock samples location
Sedimentary rock samples location
Fault
Lithology boundary
Bailingshan complex
Aqikekuduke Fault
Fig. 4M
Central Tianshan Terrane

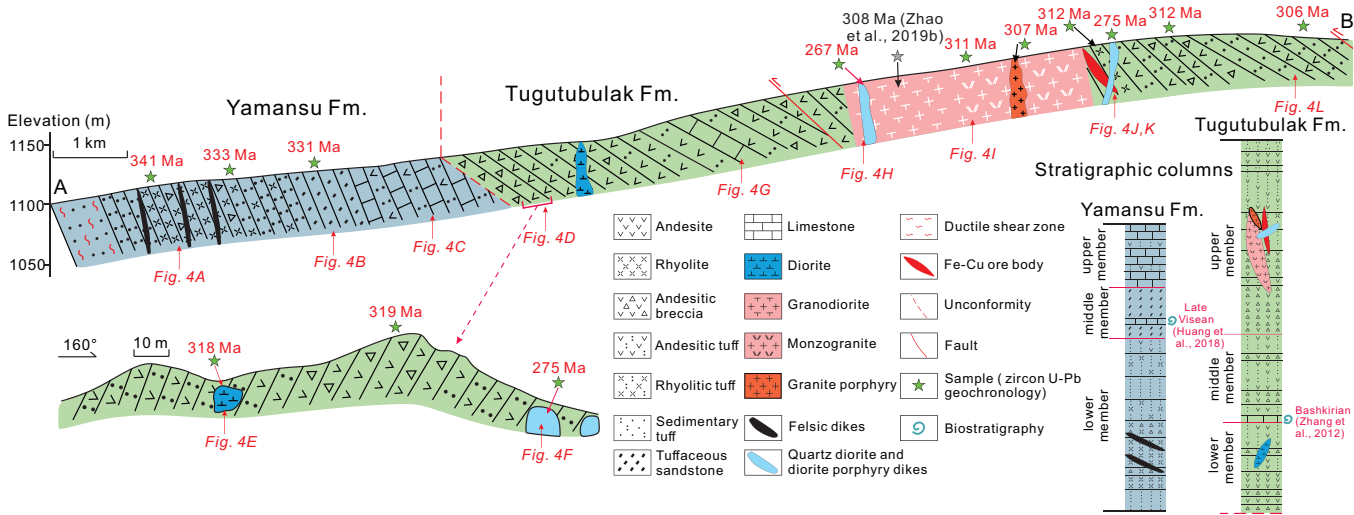
Elevation (m)
1150
1100
1050
1 km
A
B
Yamansu Fm.
Tugutubulak Fm.
341 Ma
333 Ma
331 Ma
308 Ma (Zhao et al., 2019b)
267 Ma
311 Ma
307 Ma
312 Ma
275 Ma
312 Ma
306 Ma
Fig. 4A
Fig. 4B
Fig. 4C
Fig. 4D
Fig. 4E
Fig. 4F
Fig. 4G
Fig. 4H
Fig. 4I
Fig. 4J,K
Fig. 4L
160°
10 m
319 Ma
318 Ma
275 Ma
Andesite
Rhyolite
Andesitic breccia
Andesitic tuff
Rhyolitic tuff
Sedimentary tuff
Tuffaceous sandstone
Limestone
Diorite
Granodiorite
Monzogranite
Granite porphyry
Felsic dikes
Quartz diorite and diorite porphyry dikes
Ductile shear zone
Fe-Cu ore body
Unconformity
Fault
Sample (zircon U-Pb geochronology)
Biostratigraphy
Stratigraphic columns
Yamansu Fm.
upper member
middle member
lower member
Late Visean (Huang et al., 2018)
Tugutubulak Fm.
upper member
middle member
lower member
Bashkirian (Zhang et al., 2012)


A
Kangguer shear zone
Rhyolite
(Yamansu Formation)
Obsidian dike
B
Fig. 4D
Fig. 4C
Tuffaceous sandstone
C
Limestone
(Yamansu Fm.)
Andesitic tuff
20 cm
D
Yamansu Formation
5 m
Tugutubulak Formation
Fig. 4E
Fig. 4F
E
Andesitic tuff
Diorite
30 cm
F
Andesite
1 m
Diorite porphyry
G
Andesitic tuff
Limestone
(Tugutubulak Fm.)
50 cm
H
Quartz diorite
Granodiorite
I
Monzogranite
Granodiorite
J
Hematite-sulfide
(chalcopyrite)
orebody
Andesitic tuff
(Epidote alteration)
1 m
K
Diorite porphyry
Magnetite
orebody
Andesitic tuff
L
Andesite
Sedimentary tuff
1 m
M
Central Tianshan Terrane
Aqikekuduke fault
Tugutubulak Formation
50 m

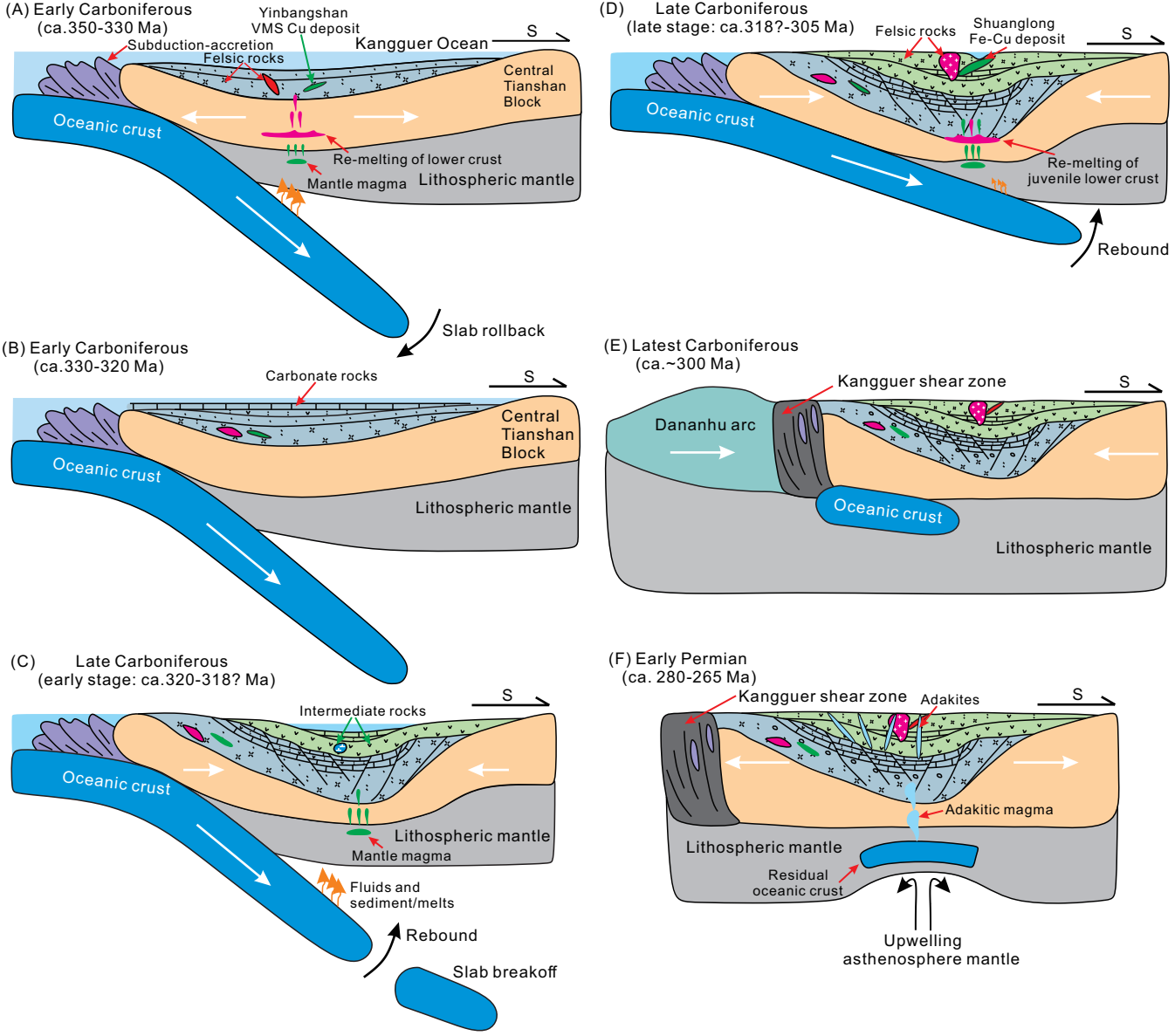
(A) Early Carboniferous
(ca.350-330 Ma)
Yinbangshan
VMS Cu deposit
Subduction-accretion
Felsic rocks
Kangguer Ocean
S
Central
Tianshan
Block
Oceanic crust
Re-melting of lower crust
Mantle magma
Lithospheric mantle
Slab rollback
(B) Early Carboniferous
(ca.330-320 Ma)
Carbonate rocks
S
Central
Tianshan
Block
Oceanic crust
Lithospheric mantle
(C) Late Carboniferous
(early stage: ca.320-318? Ma)
S
Intermediate rocks
Oceanic crust
Lithospheric mantle
Mantle magma
Fluids and
sediment/melts
Rebound
Slab breakoff
(D) Late Carboniferous
(late stage: ca.318?-305 Ma)
Felsic rocks
Shuanglong
Fe-Cu deposit
S
Oceanic crust
Re-melting of
juvenile lower crust
Rebound
(E) Latest Carboniferous
(ca.~300 Ma)
Kangguer shear zone
S
Dananhu arc
Oceanic crust
Lithospheric mantle
(F) Early Permian
(ca. 280-265 Ma)
Kangguer shear zone
Adakites
S
Adakitic magma
Lithospheric mantle
Residual
oceanic crust
Upwelling
asthenosphere mantle